Journal of Control, Automation and Electrical Systems (2020) 31:1499–1507
https://doi.org/10.1007/s40313-020-00632-6

Demand Side Management Strategy for Distribution Networks Volt/Var Control: A FCS-Model Predictive Control Approach

Rafael A. Fuhrmann[1] · Raul V. A. Monteiro[1] · Surya C. Dhulipala[2] · Arturo Bretas[2]

Received: 17 January 2020 / Revised: 20 June 2020 / Accepted: 3 August 2020 / Published online: 11 August 2020

Abstract

Due to the advent of distributed energy resources at distribution level, utility companies face new challenges in terms of voltage control. Existing works in the literature have proposed the use of demand side management (DSM) to provide ancillary services to the grid. Some works explored the use of thermal inertia of buildings to tackle the frequency regulation problem. Existing DSM strategies ignore the potential service loads can provide for the Volt/Var control (VVC) problem. The ability of smart buildings to provide reactive power support to the grid has not been exploited to date. In this paper, we present a finite control state model predictive control strategy for VVC in distribution networks. The robustness of this strategy is validated on a modified IEEE 13 bus system.

Keywords Demand side management · FCS-MPC · Smart grids

1 Introduction

Demand side management (DSM) is a strategy in which the consumer side, i.e. residential, industrial and commercial loads, is modulated to provide ancillary services to the grid, to maintain the voltage magnitude and frequency levels in allowable operational region (Palensky and Dietrich 2011).

At distribution level, some common DSM strategies range from load shifting (flattening action over the grid's load profile) to direct load control (DLC)—an approach in which the operator is able to curtail (load shedding) or modulate individual loads' consumption (DSM) to meet the grid's needs at the time (Palensky and Dietrich 2011).

In this work, we present a DLC method which modulates power consumption of thermostatically controlled loads (TCLs)—heating, ventilation and air conditioning systems (HVAC) in this case. HVACs are suitable candidates for DSM due to their inherent thermal energy storage capabilities. DLC for Volt/Var control (VVC) was explored in our previous work of Dhulipala et al. (2018) which uses the priority stack controller, where an agent changes the state of operation (ON/OFF) of an optimal number of HVAC systems in order to restore the distribution network (DN) voltage profile to nominal levels. HVACs are also suitable for load balancing services, as demonstrated by Lu (2012). Other successful examples can be found in the works of Lampropoulos et al. (2013), Bomela et al. (2018) and Mahdavi et al. (2017).

There is a need for proper control technique to completely tackle the DLC problem. One such method is the model predictive control (MPC), a methodology where an online optimization problem is solved over a receding horizon based on the controlled plant model predictions to track a desired trajectory (Sultana et al. 2017). A branch of MPC, the finite control set model predictive control (FCS-MPC) presents an MPC version suitable for systems with finite control possibilities, such as power converters (Aguilera et al. 2013; Singh et al. 2018; Ramírez et al. 2019).

This paper tackles the problem of VVC in DN by DLC of HVAC systems. To achieve that objective, a local FCS-MPC was developed to control the HVAC systems temperature set point in order to track reference signals sent by an agent whenever voltage violations occur (upwards and downwards regulation).

✉ Raul V. A. Monteiro
raulvitoramonteiro@gmail.com

Rafael A. Fuhrmann
rafael.afh@gmail.com

Surya C. Dhulipala
chandandhulipala@ufl.edu

Arturo Bretas
arturo@ece.ufl.edu

1 Federal University of Mato Grosso, Cuiabá, Brazil

2 University of Florida, Gainesville, USA

The remainder of the paper is organized as follows: Sect. 2 presents a brief overview of the state of the art of DSM applied to VVC. Section 3 presents the techniques used, the FCS-MPC formulation and its application to HVAC control as well as an overview of the proposed system architecture. The simulations parameters and results are shown in Sects. 4 and 5 provides some concluding remarks.

2 Motivation and Background

The use of DSM techniques for VVC in DN control has been a field of interest in recent years. The authors in Zakariazadeh et al. (2014) applied an emergency DSM program for real-time voltage control. This method uses real-time data from remote terminal units to determine the tap changer operation and load curtailment. The results showed a reduction on voltage drops and a boost in voltage level on the feeder ends.

In Bhattarai et al. (2015), over-voltage in DNs with high photovoltaic (PV) penetration is dealt with a demand response technique which coordinates load modulation and PV generation. Electrical vehicles (EV) were used as a DR resource, with its charging state being controlled to increase PV's utilization. Their proposal was verified by a simulation of a Danish DN and the obtained results demonstrated improvements in the technical and economical performance. In Yang and Tan (2016), an electric coil is applied together with a smart load as a strategy for voltage and frequency regulation, where the smart load was able to provide regulation without conventional communication requirements. Simulations were carried out on a modified version of the IEEE 13-node test feeder and the proposed system was able to maintain voltage and frequency regulation, whereas the conventional control could not. Also, the authors provided some experimental results validating the proposal. An incentive-based algorithm was developed by Zhou et al. (2017), to ensure that the voltage profile remained inside desired boundaries, while both consumers and operator objectives are taken in consideration. The authors formulated this as a convex programming problem with an incentive signal strategy. This methodology was tested via a simulation of the IEEE 37-node test feeder, running a nonlinear AC power flow and the control was able to maintain the voltage within the allowable boundaries. In Luo et al. (2017), an electrical coil was used to turn an ice-thermal storage unit in a smart building to provide VVC with a DR technique. The authors first developed a building energy model based on real measurements that incorporates the aforementioned three-phase electric spring. By means of an experimental assembly with a programmable source intended to emulate a feeder including intermittent generation and computational simulations, the proposed methodology was validated, as the smart load adapted its thermal load to absorb power fluctuations and maintain the voltage profile close to the desired value.

In Olival et al. (2017), an algorithm was developed to control the voltage on a low-voltage (LV) network with distributed energy resources (DER), such as residential loads. In their methodology, a hourly simulation was used to account for voltage violations, using load and energy production forecast profile. Then, an evolutionary particle swarm optimization (EPSO) was used to evaluate possible control events, which consists on actions such as non-critical residential load shedding or generation curtailment. The methodology described above was tested against a Portuguese LV grid, where voltage profile deviations were successfully mitigated. A two-stage hierarchical voltage–load sensitivity matrix (VLSM)-based DR algorithm was proposed by Zhu et al. (2018) for voltage regulation on distribution feeders. In the proposed methodology, transmission-level DR requests are used to trigger distribution level dispatch of DR resources to minimize voltage deviations and a second dispatch may occur if voltage deviations remain. The aforementioned algorithm was validated by means of simulations using the IEEE 123-node test feeder, where smart PV inverters, controllable loads and capacitor banks were used as DR resources. The problem of regulating voltage in LV grids with high PV penetration was also tackled by Wang et al. (2018). A hierarchical dispatch strategy is employed to coordinate multiple aggregators, each of them aggregating residential air-conditioners with a localized control. A consensus approach is used for the coordination of the aggregators. To validate that proposal, the authors carried simulations on a LV feeder composed of six nodes, taken from the IEEE 15 bus distribution network, whose voltages were successfully controlled and maintained inside allowable boundaries.

In Hashemi et al. (2018), the authors present an algorithm for optimal load reduction in a DR program to retain the voltage level at a security margin. Firstly, a threshold voltage is estimated and the system operator is notified in order to take appropriate measures; then, if there is no sufficient voltage stability margin, a load reduction action is taken by means of DR, where the solution of an optimization problem estimates the load reduction needed. Finally, the algorithm was validated through simulations of the New England 39-bus test feeder. Voltage unbalance was tackled by Çimen and Çetinkaya (2018), where the authors proposed an algorithm that uses TCLs as DSM resources. In this proposal, the algorithm monitors each phase voltage and its unbalance factor, until it passes a threshold value. Then, the most unbalanced phase is detected and random TCLs are turned off until the unbalance factor goes below the allowable limit. That methodology was tested through simulations of a unbalanced microgrid and it was able to reduce the unbalances. Other examples of works that dealt with VVC using DSM

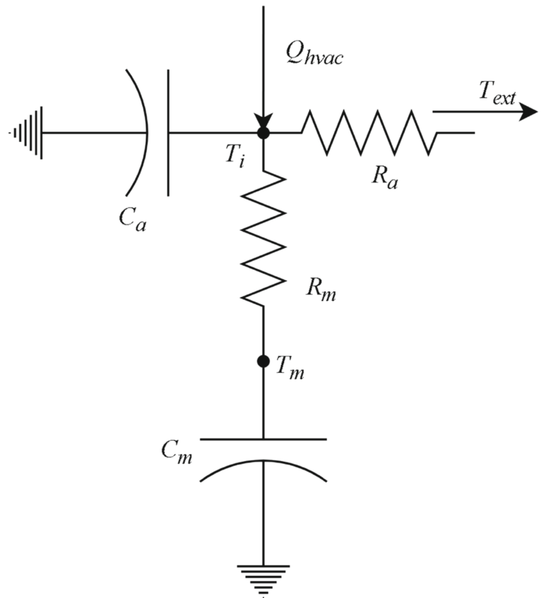

Fig. 1 Equivalent thermal parameters model representation

can be found in Tang (2018), Rahman et al. (2018), Sami et al. (2018), Acharya et al. (2019) and Lai et al. (2019).

Considering the aforementioned works, one can note that none consider the use of FCS-MPC to provide DSM for Volt/Var control in DNs. This work presents an online control of HVACs using FCS-MPC, to tackle the problem of voltage violations, considering both upwards and downwards regulation scenarios. The contributions of this work towards the state-of-the-art are:

- Formulation of DSM strategy using FCS-MPC to control TCLs (specifically HVACs);
- Use of a heterogeneous load population to give a more realistic perspective;
- VVC considering downwards and upwards regulation.

3 System Architecture and Control Overview

3.1 Equivalent Thermal Parameters Model

The approach adopted to model each HVAC consumption is the thermo-dynamic model of the room. The thermal dynamics can be represented by an electrical circuit model, using the equivalent thermal parameters model (ETP). In this work, a second-order ETP is used; its schematic representation is shown in Fig. 1 (Lu 2012).

A state-space representation of Fig. 1 is given by (1)–(5).

$$\dot{\mathbf{x}} = \mathbf{A}\mathbf{x} + \mathbf{B}\mathbf{u} \tag{1}$$

$$\mathbf{y} = \mathbf{C}\mathbf{x} + \mathbf{D}\mathbf{u} \tag{2}$$

$$\mathbf{x} = \begin{bmatrix} T_{\text{i}} \\ T_{\text{m}} \end{bmatrix}, \dot{\mathbf{x}} = \begin{bmatrix} \dot{T}_{\text{i}} \\ \dot{T}_{\text{m}} \end{bmatrix}, \mathbf{C} = \begin{bmatrix} 1 & 0 \\ 0 & 1 \end{bmatrix}, \mathbf{D} = \begin{bmatrix} 0 \\ 0 \end{bmatrix}, u = 1 \tag{3}$$

$$\mathbf{A} = \begin{bmatrix} -\left(\frac{1}{R_{\text{m}}C_{\text{a}}} + \frac{1}{R_{\text{a}}C_{\text{a}}}\right) & \frac{1}{R_{\text{m}}C_{\text{a}}} \\ \frac{1}{R_{\text{m}}C_{\text{m}}} & -\frac{1}{R_{\text{m}}C_{\text{m}}} \end{bmatrix} \tag{4}$$

$$\mathbf{B} = \begin{bmatrix} \frac{T_{\text{out}}}{R_{\text{a}}C_{\text{a}}} + \frac{Q_{\text{hvac}}}{C_{\text{a}}} \\ 0 \end{bmatrix} \tag{5}$$

where

- T_{i} and T_{m} are, respectively, the internal air room temperature and mass temperature;
- R_{a} and R_{m} are, respectively, the equivalent air and mass thermal resistances;
- C_{a} and C_{m} are, respectively, the equivalent air and mass thermal capacitances;
- Q_{hvac} is the equivalent heat flux delivered by the HVAC.

3.2 Finite Control Set Model Predictive Control

Model predictive control is a control method where a system's mathematical description, such as the one expressed in discrete time by (6)–(7), is used to forecast its behaviour in a moving time-window, usually called the receding horizon, and then those predictions are applied to a cost function that tracks a reference signal, whose solution gives an optimal set of control actions from which only the first element is used as the next control input. In other words, the MPC translates a control problem into an online optimization problem, which is capable of taking into account system nonlinearities and constraints in a straightforward manner (Sultana et al. 2017).

$$\boldsymbol{x}_{k+1} = \boldsymbol{A}\boldsymbol{x}_k + \boldsymbol{B}\boldsymbol{u}_k \tag{6}$$

$$\boldsymbol{y}_k = \boldsymbol{C}\boldsymbol{x}_k + \boldsymbol{D}\boldsymbol{u}_k \tag{7}$$

where

- $\boldsymbol{x}_k$ is the discrete state variable;
- $\boldsymbol{A}$, $\boldsymbol{B}$ and $\boldsymbol{C}$ are the system matrices in discrete time;
- $\boldsymbol{y}_k$ is the system output;
- As in MPC one control action may only produce effects in the next time-step, $D = 0$; hence, no mapping of u is made directly to the output.

Widely employed on power converters, the FCS-MPC is an adaptation of the traditional MPC to the context of systems that only have a finite set of possible control actions, thus reducing the original optimization problem into finding which control action among those available will lead the system's output closer to a desired trajectory, considering one-step ahead predictions and unchanged parameters (Kouro et al. 2009). Examples of its applications can be found in Aguilera et al. (2013), Singh et al. (2018) and Ramírez et al. (2019).

Cost functions may be simplified to decision functions (Kouro et al. 2009; Sultana et al. 2017). In that sense, based on model predictions, the control logic will choose an appropriate control action, thus diminishing computational burdens involved. This paper deals with only three possible choices that are further explained in Sect. 3.4.

3.3 Voltage Sensitivity Matrix and System Overview

In this strategy, we assume that, each phase of a Bus k has an agent which monitors the bus voltage and dispatches control (reference) signals to each available load when a voltage violation is detected, i.e. it is above 1.05 p.u. or below 0.95 p.u. To decide how many loads, and therefore how much VAR is required to mitigate the violation can be estimated the agent by using Eq. (8). Until the under-voltage or over-voltage event concludes, the agent dispatches loads needed at each time-step. Figure 3 illustrates the aforementioned process.

$$Q_{t+1} = Q_t + \frac{V_{\text{reference}} - V_{\text{measurement}}}{S_{\text{V}\Delta Q_{ij}}} \tag{8}$$

where

- Q_{t+1} and Q_t are the estimated reactive power required at t and $t+1$;
- $V_{\text{reference}}$ is the reference voltage (0.95 p.u. or 1.05 p.u);
- $V_{\text{measurement}}$ is the voltage measured at bus i;
- $S_{\text{V}\Delta Q_{ij}}$ is the sensitivity of voltage at bus i to reactive power injection at bus j.

Further developments are found in the works of Dhulipala et al. (2018). The proposed control architecture, illustrated by Figs. 2 and 4, comprises a set of HVACs equipped with local FCS-MPCs that individually receives a reference signal when a voltage event occur, that modulates its consumption by solving its internal cost function, therefore leading to an optimal temperature set point value that is fed into the thermostat, which controls the switching state of the HVAC. The aforementioned state is relayed to the agent at each time-step so it is aware of which loads are available to receive a control signal and those which are not in the next time-step, i.e. those in ON for upwards regulation and OFF for downwards regulation.

3.4 FCS-MPC Applied to HVAC Control

The crux of the application of the FCS-MPC to HVAC control is defining the control set. In this approach, the thermostat set

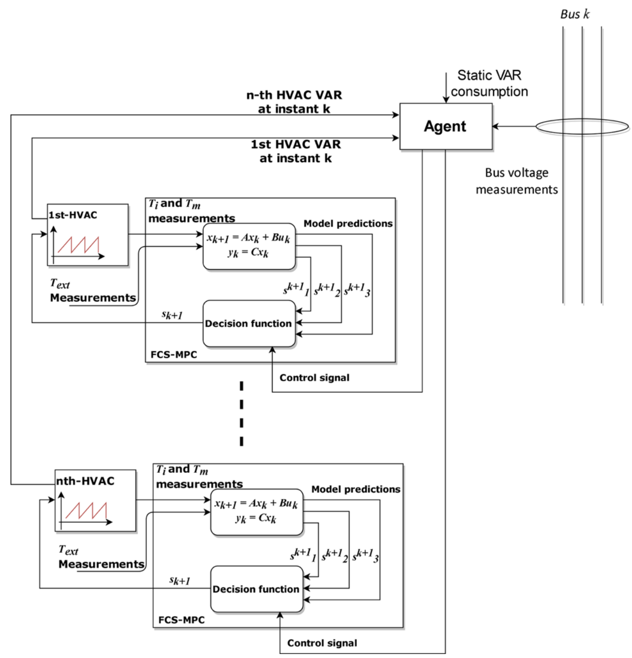

Fig. 2 System architecture overview

point is controlled to operate under only three possible control actions: raising the set point by 2 °C; lowering it by 2 °C; or maintaining its previous value. In this sense, (9) denotes the adopted thermostat model, whose actuation directly controls the HVAC output.

$$s_k = \begin{cases} 0, & \text{if } T_i \geq T_{\text{setpoint}} + \frac{\text{db}}{2} \\ 1, & \text{if } T_i \leq T_{\text{setpoint}} - \frac{\text{db}}{2} \\ s_{k-1}, & \text{otherwise} \end{cases} \tag{9}$$

$$Q_{\text{output}}^k = s_k Q_{\text{rated}} \tag{10}$$

where

- T_{set} is the thermostat set point;
- db is the dead band of HVAC system;
- Q_{output} is the VAR demand of HVAC system k;
- Q_{rated} is the VAR rating of HVAC system.

As stated in (9), the difference between the two switching limits defines the interval in which the load will be in its ON or OFF states; hence, the modulation of the set point offers a way to control the reactive power in accordance to (10), allowing to maintain the bus voltage profile inside imposed boundaries in accordance to (8). The following steps outline the control process for each one of the HVAC systems:

1. The internal room temperature at $t+1$ (T_{t+1}) is forecasted by solving a discrete version of (1)–(5).

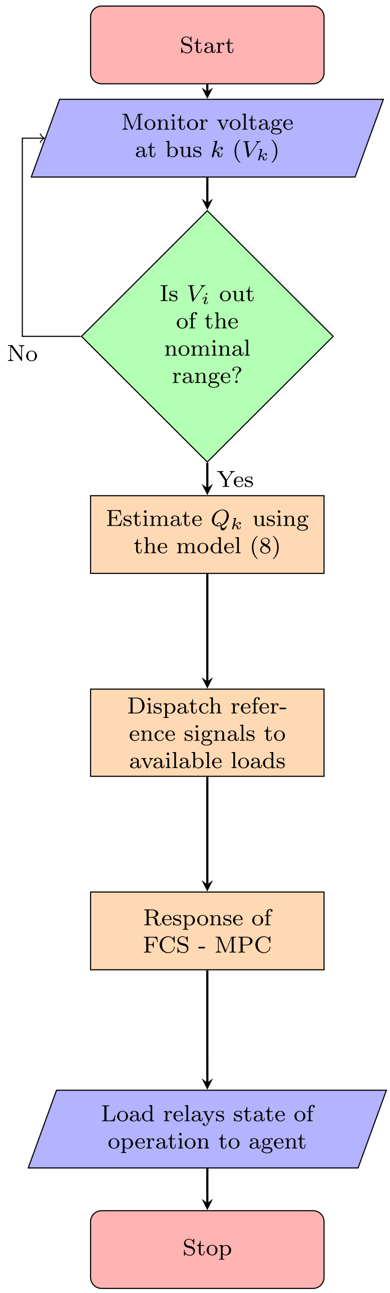

Fig. 3 Flowchart of the control actuation

2. For the predicted temperatures, evaluate s^1_{k+1}, s^2_{k+1} and s^3_{k+1} according to (9), in where each s represents a control action to be evaluated by the decision function;
3. For each s above, a control action is made considering agent reference signal—there are three possibilities;
   - 1, meaning that downwards regulation is needed thus leading to the necessity of the load having a longer cycle;
   - -1, the same as the previous one, but considering an upwards regulation and smaller cycles.

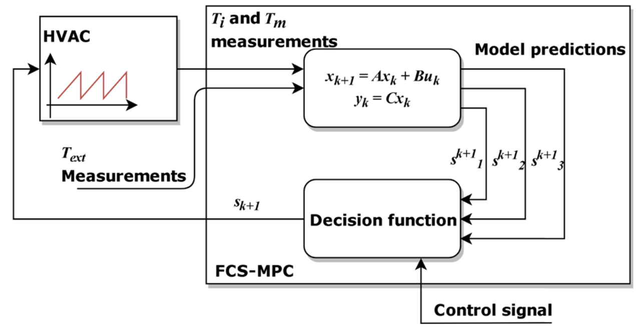

Fig. 4 FCS-MPC block diagram

   - 0, which means that no reference signal is being applied;
4. The new temperature set point is relayed to the thermostat.

After the conclusion of control actuation (i.e. voltage levels are back inside of the desired boundaries), the agent will send a zero-value reference (step 3) and each FCS-MPC will set the controlled HVAC's set point back to the initial, user-defined, value. However, in order to avoid a load synchronization that can possibly deteriorate the voltage profile of grid, the agent will send the aforementioned signals to each load at a 5-min interval. Finally, thermal comfort level constraints are considered through a saturation approach, over which maximum and minimum temperature set points are defined as to not interfere with customer comfort. Therefore, (11).

$$T^{\min}_{\text{setpoint}} \leq T_{\text{setpoint}} \leq T^{\max}_{\text{setpoint}}. \tag{11}$$

It is important to state here that some DSM strategies applied by real companies worldwide are focused on turn on and off TCL indefinitely, without any quality-of-service (QoS) constraints. As an example, one can cite the company Energex, from Australia, which offers financial rewards for consumers who join its peak demand control program. Therefore, in this research, a set point change is made in a way of just change the TCL work cycle thus not affecting the QoS so much.

4 Validation

Consider the IEEE 13 Test Feeder System MATLAB Simulink, MATLAB (2017a), model illustrated in Fig. 5. A modified version of the IEEE 13-node test feeder (no capacitor banks and dynamic loads) was simulated to test the proposed methodology with a heterogeneous population of 40 HVACs (heating mode) at phases B and C, whose parameters are summarized in Table 1. In order to achieve said heterogeneity, the

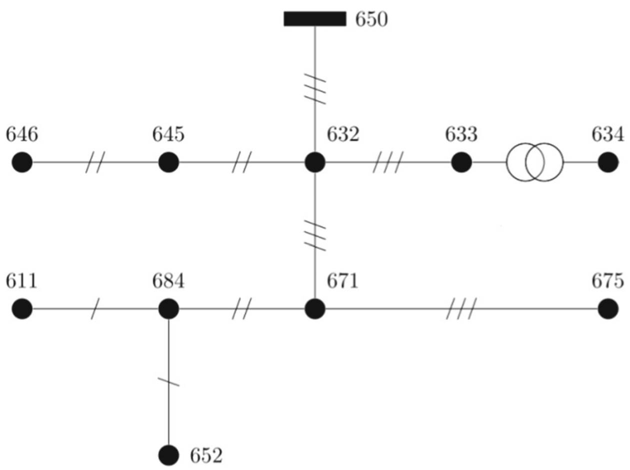

Fig. 5 IEEE 13-node test feeder topology

Table 1 Simulation parameters

Parameter	Mean value	Standard deviation	Unit
T_{set}	24	–	°C
db	2	–	°C
R_{a}	0.01208	0.005	°C/W
R_{m}	0.001208	0.0005	°C/W
C_{a}	89,975	25,000	J/°C
C_{m}	3599	1000	J/°C

ETP parameters were sampled from a log norm distribution. Initial temperatures and ON/OFF states were also randomized. However, we assumed all HVACs have the same initial temperature set point, dead band besides the same rated active and reactive power (4 KW and 3.921 KVar, respectively). The bus chose to be controlled is bus 675 from the referred system. This bus was chosen in order to achieve a greater voltage rise and drop (Gaunt and Namaya 2017). All results showed are related to this bus parameters. In addition to that, the model (1)–(5) was discretized with a 1-min time-step.

4.1 Simulation Results and Discussion

The simulation results are shown in the subsequent subsections. Each HVAC internal temperature without any control signal is shown in Fig. 6.

4.2 Upwards Regulation Case

Figure 7 shows the bus voltages for the case where no control action occurs, with lower voltage boundary (represented by the purple line) violation at phase C. Figures 9 and 11 illustrate the internal rooms' temperatures and bus voltages, respectively, for the controlled case. The P–Q curves for the

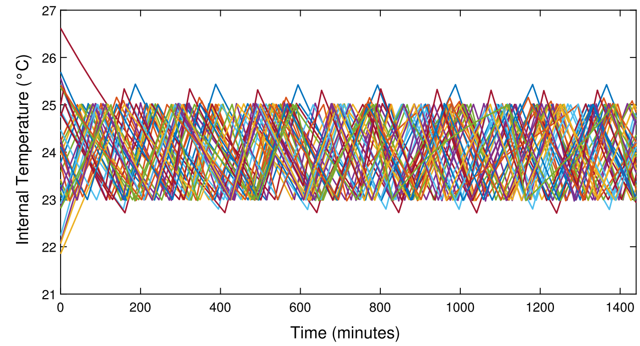

Fig. 6 Internal room temperatures when no reference signal is sent

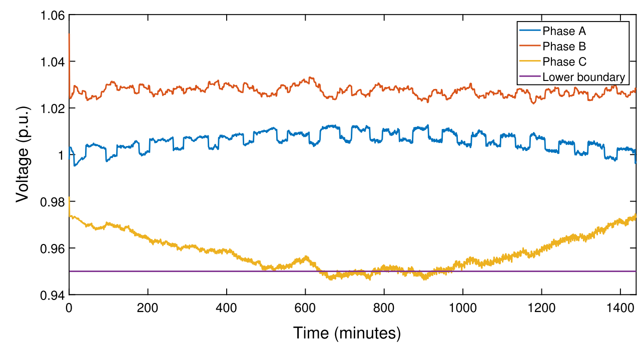

Fig. 7 Phase C uncontrolled bus voltage

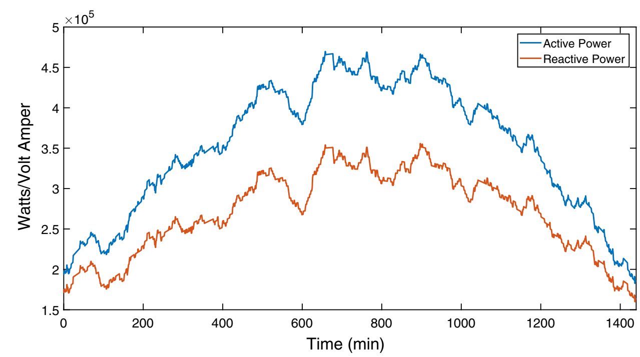

Fig. 8 Phase C P–Q curves: uncontrolled under-voltage case

uncontrolled and the controlled case are shown in Figs. 8 and 10, respectively.

As one can see from Fig. 9, the control strategy restores phase C voltage to the allowable region. To achieve that, each load that received a reference signal from the agent changed its' set point leading to the trajectories shown in Fig. 11. Figure 12 shows the load actuations and the estimated and required VAR for upwards regulation, in response to a voltage event initiated at minute 524 and ended at minute 1164. It can be seen that when the required amount of reactive power increased, more loads actuations were performed by relaying the reference signal, thus providing more reactive power support to regulate the voltage level, until it was restored to allowable region.

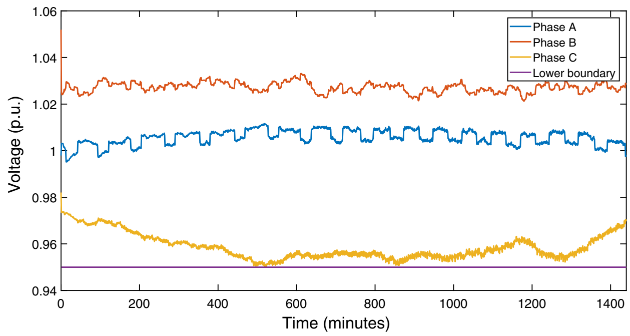

Fig. 9 Phase C controlled bus voltage

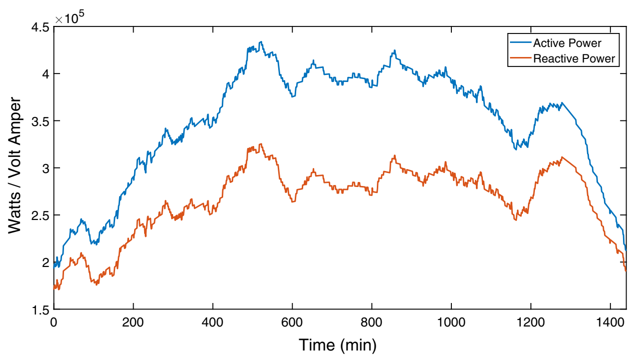

Fig. 10 Phase C P–Q curves: controlled under-voltage case

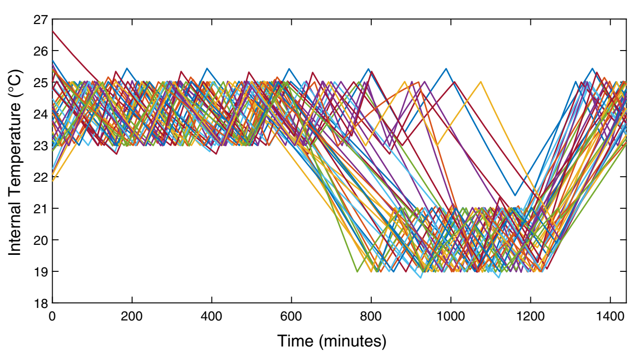

Fig. 11 Internal rooms' temperatures in the phase C controlled case

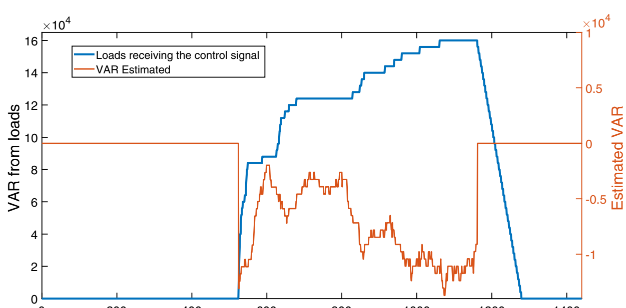

Fig. 12 Load actuation and estimated required VAR for upwards regulation

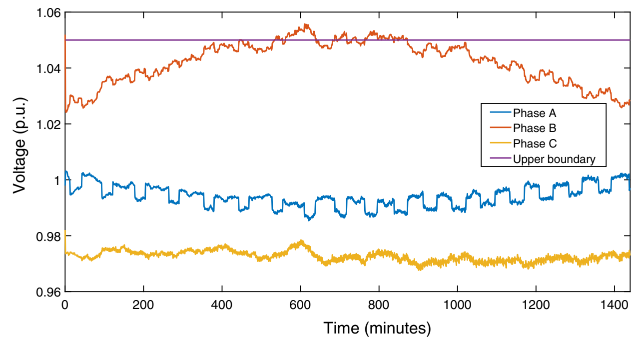

Fig. 13 Phase B uncontrolled voltage

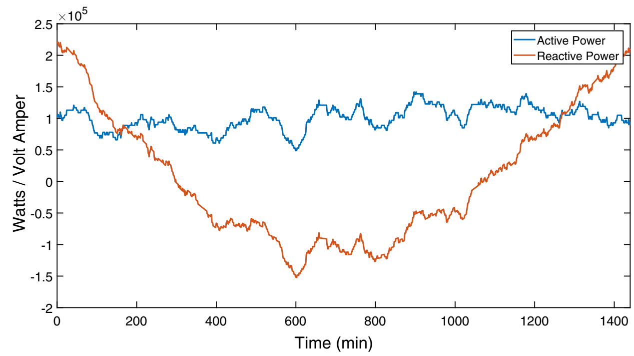

Fig. 14 Phase C P–Q curves: uncontrolled over-voltage case

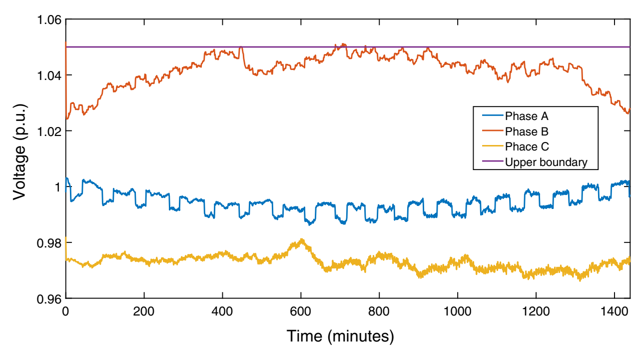

Fig. 15 Phase B controlled voltage for downwards regulation

4.3 Downwards Regulation Case

As for the over-voltage event case, uncontrolled and controlled bus voltage for phase B scenarios are shown in Figs. 13 and 15, respectively. The P–Q curves for the uncontrolled and the controlled case are shown in Figs. 14 and 16, respectively.

The room temperatures trajectory for this scenario is shown in Fig. 17, showing the impact on the temperatures caused by the response to the control.

As one can see, each load responded by increasing its' set point in order to increase their consumption and therefore absorbing more reactive power from the grid. Therefore, the voltage at phase B was restored below 1.05 p.u., the boundary represented by the purple line in Fig. 15. Also, Fig. 18 shows

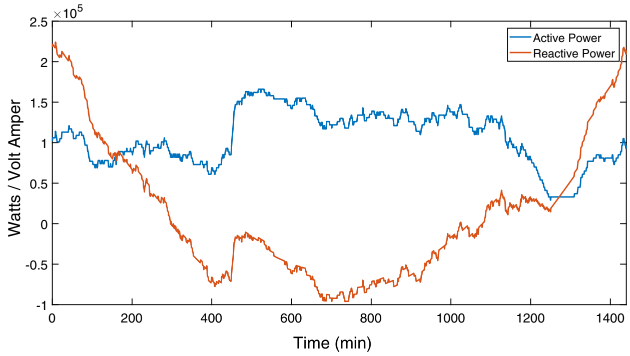

Fig. 16 Phase C P–Q curves: controlled over-voltage case

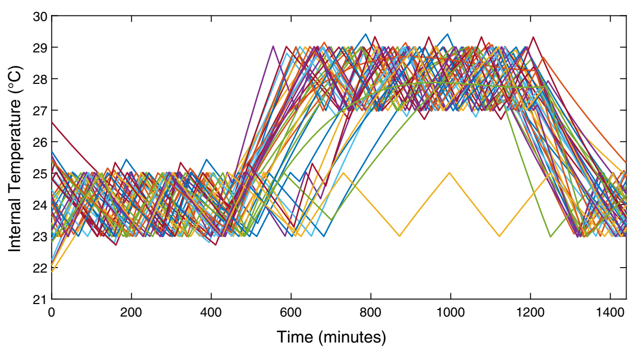

Fig. 17 Internal room temperatures in the controlled over-voltage case, phase B

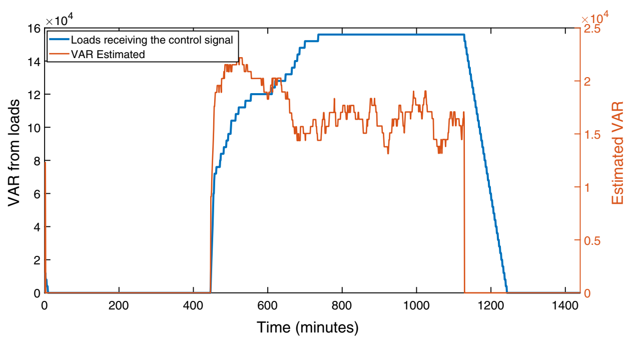

Fig. 18 Load activation and estimated required VAR for downwards regulation

the loads being controlled as the required VAR increased. In this case, for downwards regulation, we need the HAVC systems to consume more reactive power from the grid to restore the bus voltage profile inside allowable ranges. Finally, as in the under-voltage scenario, the control was sustained until the voltage came back to the desired limits.

4.4 Control Effectiveness Analysis

In order to test the effectiveness of the proposed control method, each violation length of time as a percentage of total simulated time was calculated for both, controlled and uncontrolled cases, for both under and over-voltage case. Those results are summarized in Table 2. It can be seen there is a reduction in the amount of time violation occurs for the controlled case when compared to uncontrolled case.

Table 2 Violation duration as a percentage of total simulated time

	Uncontrolled (%)	Controlled (%)	Reduction (%)
Under-voltage	14.6	0.1	99.3
Over-voltage	18.3	2.6	85.8

A bus operational condition in a distributed energy system, are defined in terms of its magnitude and frequency. However, this research is focused only on the control efficiency and viability. Therefore, power quality indices are not carried out in the analysis.

Despite other strategies that uses the idea of turning ON/OFF thermostatically controlled loads, the one presented herein takes into account the QoS, and preserves, in certain level, the consumer's room temperature. On the other hand, the set point changing of the HVACs could decrease their lifetime. However, compared to ON/OFF strategies, this research presented can considerably not decrease the HVACs lifetime, once it affects the set point preserving their dead band, thus letting them working normally.

5 Conclusions

This paper investigates the problem of voltage regulation in a distribution network. A DSM strategy to provide the required VAR to mitigate voltage magnitude violations, such as under- and over-voltage, using FCS-MPC control for HVAC systems was proposed. For VVC, an agent estimates the required amount of VAR to be absorbed or injected into a grid and then select an adequate amount of HVAC systems that can locally respond to provide reactive power support to the grid by changing their state of operation.

With the advantage of dealing with a finite set of cost functions (which is a characteristic of control of HVAC systems), the FCS-MPC is an interesting candidate to mitigate VVC problems in DNs. This method can be also used with other TCLs with a different set of control rules. Future works will expand the proposed methodology with a consensus approach.

References

Acharya, S., El-moursi, M. S., Al-hinai, A., Al-sumaiti, A. S., & Zeineldin, H. H. (2019). A control strategy for voltage unbalance mitigation in an islanded microgrid considering demand side management capability. *IEEE Transactions on Smart Grid*, *10*(3), 2558–2568.

Aguilera, R. P., Lezana, P., & Quevedo, D. E. (2013). Finite-control-set model predictive control with improved steady-state performance. *IEEE Transactions on Industrial Informatics*, *9*(2), 658–667.

Bhattarai, B. P., Bak-jensen, B., Pillai, J. R., Gentle, J. P., & Myers, K. S. (2015). Overvoltage mitigation using coordinated control of demand response and grid-tied photovoltaics. In *2015 IEEE conference on technologies for sustainability (SusTech)* (pp. 83–89).

Bomela, W., Zlotnik, A., & Li, J. S. (2018). A phase model approach for thermostatically controlled load demand response. *Applied Energy*, *228*, 667–680.

Çimen, H., & Çetinkaya, N. (2018). Mitigation of voltage unbalance in microgrids using thermostatically controlled loads. In *2018 2nd international symposium on multidisciplinary studies and innovative technologies (ISMSIT)* (pp. 1–4).

Dhulipala, S. C., Ruben, C., Bretas, A., Monteiro, R. V. A., & Guimarães, G. C. (2018). A distributed strategy for volt/var control in distribution networks: A smart buildings approach. In *2018 North American power symposium (NAPS)* (pp. 1–6).

Gaunt, C. T., & Namaya, R. H. E. (2017). Voltage modelling of LV feeders with dispersed generation: Limits of penetration of randomly connected photovoltaic generation. *Electric Power Systems Research*, *143*, 1–6.

Hashemi, S., Aghamohammadi, M. R., & Sangrody, H. (2018). Electrical power and energy systems restoring desired voltage security margin based on demand response using load-to-source impedance ratio index and PSO. *Electrical Power and Energy Systems*, *96*, 143–151.

Kouro, S., Cortes, P., Vargas, R., Ammann, U., & Rodriguez, J. (2009). Model predictive control—A simple and powerful method to control power converters. *IEEE Transactions on Industrial Electronics*, *56*(6), 1826–1838.

Lai, J., Lu, X., Rl, Tang, Li, X., & Dong, Z. (2019). Delay-tolerant distributed voltage control for multiple smart loads in AC microgrids. *ISA Transactions*, *86*, 181–191.

Lampropoulos, I., Baghină, N., Kling, W. L., & Ribeiro, P. F. (2013). A predictive control scheme for real-time demand response applications. *IEEE Transactions on Smart Grid*, *4*(4), 2049–2060.

Lu, N. (2012). An evaluation of the HVAC load potential for providing load balancing service. *IEEE Transactions on Smart Grid*, *3*(3), 1263–1270.

Luo, X., Member, S., Lee, C. K., Member, S., Ng, W. M., Yan, S., et al. (2017). Use of adaptive thermal storage system as smart load for voltage control and demand response. *IEEE Transactions on Smart Grid*, *8*(3), 1231–1241.

Mahdavi, N., Braslavsky, J. H., Seron, M. M., & West, S. R. (2017). Model predictive control of distributed air-conditioning loads to compensate fluctuations in solar power. *IEEE Transactions on Smart Grid*, *8*(6), 3055–3065.

MATLAB. (2017a). *Matlab version 8.9(r2017a)*. Natick: The Mathworks, Inc.

Olival, P. C., Madureira, A. G., & Matos, M. (2017). Advanced voltage control for smart microgrids using distributed energy resources. *Electric Power Systems Research*, *146*, 132–140.

Palensky, P., & Dietrich, D. (2011). Demand side management: Demand response, intelligent energy systems, and smart loads. *IEEE Transactions on Industrial Informatics, 7*(3), 381–388. arXiv:1011.1669v3.

Rahman, M., Are, A., Sha, G. M., & Hettiwatte, S. (2018). A new approach to voltage management in unbalanced low voltage networks using demand response and OLTC considering consumer preference. *Electrical Power and Energy Systems*, *99*, 11–27.

Ramírez, R. O., Espinoza, J. R., Baier, C. R., Rivera, M., Villarroel, F., Guzman, J. I., et al. (2019). Finite-state model predictive control with integral action applied to a single-phase z-source inverter. *IEEE Journal of Emerging and Selected Topics in Power Electronics*, *7*(1), 228–239.

Sami, S. S., Cheng, M., & Wu, J. (2018). A virtual energy storage system for voltage control of distribution networks. *CSEE Journal of Power and Energy Systems*, *4*(2), 146–154.

Singh, V. K., Tripathi, R. N., & Hanamoto, T. (2018). Model-based design approach for implementation of finite state MPC. In *Proceedings of the 13th IEEE conference on industrial electronics and applications, ICIEA 2018*.

Sultana, W. R., Sahoo, S. K., Sukchai, S., Yamuna, S., & Venkatesh, D. (2017). A review on state of art development of model predictive control for renewable energy applications. *Renewable and Sustainable Energy Reviews*, *76*(March), 391–406. https://doi.org/10.1016/j.rser.2017.03.058.

Tang, Z. (2018). Hierarchical voltage control of weak subtransmission networks with high penetration of wind power. *IEEE Transactions on Power Systems*, *33*(1), 187–197.

Wang, D., Member, S., Meng, K., & Gao, X. (2018). Coordinated dispatch of virtual energy storage systems in LV grids for voltage regulation. *IEEE Transactions on Industrial Informatics*, *14*(6), 2452–2462.

Yang, Y., & Tan, S. C. (2016). Voltage and frequency control of electric spring based smart loads. In *2016 IEEE applied power electronics conference and exposition (APEC)* (pp. 3481–3487).

Zakariazadeh, A., Homaee, O., Jadid, S., & Siano, P. (2014). A new approach for real time voltage control using demand response in an automated distribution system. *Applied Energy*, *117*, 157–166.

Zhou X, Anese ED, Chen L, Baker K (2017) Incentive-based Voltage Regulation in Distribution Networks. 2017 American Control Conference (ACC) pp 2732–2738

Zhu, X., Member, S., Wang, J., Member, S., Lu, N., & Member, S. (2018). A hierarchical VLSM-based demand response strategy for coordinative voltage control between transmission and distribution systems. *IEEE Transactions on Smart Grid*, *10*, 4838–4847.